JOURNAL OF FORENSIC SCIENCES

J Forensic Sci, January 2011, Vol. 56, No. S1
doi: 10.1111/j.1556-4029.2010.01628.x
Available online at: onlinelibrary.wiley.com

TECHNICAL NOTE

CRIMINALISTICS

Thomas J. Bruno,[1] *Ph.D.; Tara M. Lovestead,*[1] *Ph.D.; and Marcia L. Huber,*[1] *Ph.D.*

Prediction and Preliminary Standardization of Fire Debris Constituents with the Advanced Distillation Curve Method*

ABSTRACT: The recent National Academy of Sciences report on forensic sciences states that the study of fire patterns and debris in arson fires is in need of additional work and eventual standardization. We discuss a recently introduced method that can provide predicted evaporation patterns for ignitable liquids as a function of temperature. The method is a complex fluid analysis protocol, the advanced distillation curve approach, featuring a composition explicit data channel for each distillate fraction (for qualitative, quantitative, and trace analysis), low uncertainty temperature measurements that are thermodynamic state points that can be modeled with an equation of state, consistency with a century of historical data, and an assessment of the energy content of each distillate fraction. We discuss the application of the method to kerosenes and gasolines and outline how expansion of the scope of fluids to other ignitable liquids can benefit the criminalist in the analysis of fire debris for arson.

KEYWORDS: forensic science, advanced distillation curve, evaporation patterns, ignitable liquids, trace analysis, weathering

Fires are responsible for the loss of *c*. $6 billion annually in the United States, and *c*. $2 billion of this total is because of arson fires. Moreover, each year, an average of 500 people die in the United States in arson fires (1). The investigation of arson fires results in a surprisingly low arrest rate (*c*. 19%) and a low conviction rate (*c*. 2%), partly because of the difficulty inherent in the chemical analysis of fire debris (2). On the other hand, there is reason to think that many past convictions for arson and arson-related homicides are in fact unjustified. Indeed, there are instances in which the death penalty has been imposed for arson homicides, but subsequent analysis and examination of the evidence called the conviction into serious question (2–4). It is apparent that the area of arson investigation and fire debris analysis can benefit greatly from standard measurements conducted in a scientifically sound manner (5). A firm link to established scientific theory would also help lend reliability and credibility to analytical conclusions and opinions expressed in court.

Many ignitable liquids can be used to start an arson fire, the most common being gasoline, kerosene, charcoal lighter fluid, alcohols, paint thinners, solvents, and other less common fuels (6,7). Attention is even being paid to the new alternative fuels, such as biodiesel fuel, as potential ignitable liquids (8). Forensic scientists and criminalists must routinely identify and characterize in a credible, defensible manner the ignitable liquid or ignitable liquid used to start an arson fire. The analysis of fire debris for the presence of residual ignitable liquid has long been an accepted and routine aspect of arson investigations. The techniques available for such analyses have evolved dramatically in recent years. The application of sophisticated techniques, such as nuclear magnetic resonance spectroscopy (^{1}H and ^{13}C), fluorescence spectroscopy, second derivative ultraviolet spectroscopy, as well as gas and liquid chromatographic techniques, have been used (9–11). The nature of ignitable liquids as multicomponent, moderately volatile fluids renders the technique of gas chromatography as the most important and widely used method for fire debris analysis. Indeed, the majority of liquid residue analyses carried out in forensic labs utilize gas chromatography with some combination of detectors and peripherals (7,9,11–17).

Gas chromatographic analyses of as-purchased ignitable liquids typically produce chromatograms that are characteristic of each class of fluids. For example, gasolines and kerosenes have elution characteristics (typically presented as signal intensity plotted against retention time) that can be identified by simple pattern recognition methods (16). A typical gas chromatogram of a fresh sample of gasoline will show a pattern of isoalkanes in the early elution region, along with some straight chain aliphatics. In the elution region of seven carbons and higher, one will see a familiar aromatic pattern with methyl-, ethyl-, and dimethylbenzenes. The analysis of gasoline (and other ignitable liquids) in fire debris as presented to the analyst is far less straightforward, however. As the sample of gasoline evaporates, the chromatographic pattern will shift to the later eluting fractions. This is clearly illustrated in Fig. 1 for gasoline (12). We note that as the evaporation of gasoline is continued to dryness, the component suite shifts to heavier (usually higher molecular mass), lower vapor pressure and higher boiling point components. Moreover, the trend in composition for gasoline is toward enriching (or concentrating) the aromatics and depleting the isoalkanes. This trend is critical to understand and utilize in fire debris analysis, because ignitable liquids have a remarkable persistence when held within the interstices of porous material, even when exposed to elevated temperatures (15).

[1]Thermophysical Properties Division, National Institute of Standards and Technology, 325 Broadway, MS 838.00, Boulder, CO 80305.

Received 18 May 2009; and in revised form 14 Dec. 2009; accepted 19 Dec. 2009.

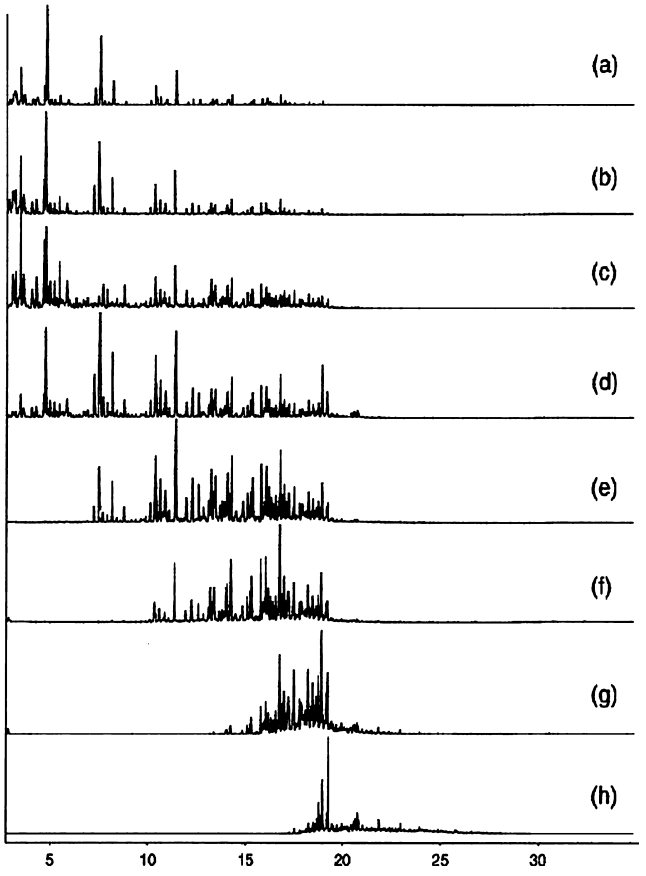

FIG. 1—*Total ion chromatograms of gasoline at various stages of evaporation presented a function of retention time in minutes: (a) fresh gasoline, (b) 25% evaporated, (c) 50% evaporated, (d) 75% evaporated, (e) 90% evaporated, (f) 95% evaporated, (g) 98% evaporated, and (h) gasoline evaporated to dryness. Reproduced with permission (12).*

The pattern shift shown in Fig. 1, while specifically for gasoline, is similar in character to that shown by any ignitable liquid. Clearly, the specific details will differ in terms of the composition suite that will be recovered after progressive evaporation, but the evaporative trend will always be noted. The evaporative trend of the sample is similar to what can be expected upon distillation of the starting fluid. In both cases, the fluid is fractionated primarily by boiling temperature and to a lesser extent by the influence of specific intermolecular interactions. What is indeed remarkable is the striking similarity of the evaporation profile of Fig. 1 with the composition explicit data channel of a recently introduced technique called the advanced distillation curve (ADC) method (18–21).

In general terms, the classical distillation curve of a fluid is a graphical depiction of the boiling temperature of the fluid mixture plotted against the volume fraction distilled (22). This volume fraction is usually expressed as a cumulative percent of the total volume. One most often thinks of distillation curves in the context of petrochemicals and petroleum refining, but such curves are of great value in assessing the properties of any complex mixture (23–25). Indeed, the measurement of distillation curves has been part of complex fluid specifications for a century (typically listed in specifications and data sheets as the fluid volatility), and they are inherent in the design of all fuels (26,27). Despite this importance, the classical methods for the measurement of such curves have been plagued with systematic uncertainty and bias, leading many petroleum engineers to consider it standardized voodoo (18,19).

The ADC differs significantly from classical distillation curve measurement. It was developed to improve the classical measurement and is an analytical protocol that can be applied to any complex fluid. It features (i) a composition explicit data channel for each distillate fraction (for both qualitative and quantitative analysis), (ii) temperature measurements that are true thermodynamic state points that can be modeled with an equation of state, (iii) temperature, volume, and pressure measurements of low uncertainty suitable for equation of state development (R. Chirico, personal communication), (iv) consistency with a century of historical data, (v) an assessment of the energy content of each distillate fraction, (vi) trace chemical analysis of each distillate fraction, and (vii) corrosivity assessment of each distillate fraction (18,19,21,28–31). The first aspect summarized earlier, the composition explicit channel, essentially provides the evaporation profile of Fig. 1, along with the distillation curve. The other features of the approach provide additional advantages applicable to the study of ignitable liquids used as ignitable liquids, however.

Relating the evaporation profile to true thermodynamic state points of the distillation curve provides a critical link to thermodynamic theory. We are able to describe the distillation curve resulting from our metrology with a model based on an equation of state (32–35). Such thermodynamic model development is simply impossible with the classical approach to distillation curve measurement, or with any of the other techniques that are used to assess fuel volatility (i.e., vapor–liquid equilibrium). The application of the ADC to the study of fuels used as arson ignitable liquids thus has the potential of validating analyses and providing a predictive framework to guide analyses of evaporated or weathered ignitable fluids absorbed in fire debris.

Materials and Methods

The apparatus used for the ADC measurement (depicted schematically in Fig. 2, with additional details provided in Figs 3 and 4) has been described in detail elsewhere, so only a brief summary will be provided here. The distillation vessel (in which the fuel sample is placed) is a round-bottom flask that is inserted in a two-part aluminum heating jacket, the lower part of which is contoured to fit the flask. Cartridge heaters are placed in the lower, contoured part of the jacket, capable of operation up to 350°C, with a local uniformity of 0.2°C. The jacket exterior is insulated with a Pyrex wool enclosure.

Three observation ports are provided in the insulation to allow penetration with a flexible, illuminated bore scope. The bore scope ports, illustrated in Fig 2, are placed to observe the fluid in the boiling flask, the top of the boiling flask (where the spherical section joins the head, and the distillation head (at the bottom of the takeoff). Above the distillation flask, a centering adapter provides access for two thermally tempered K-type thermocouples that enter the distillation head. One thermocouple (T1 in Fig. 2) enters the distillation flask and is submerged in the fluid to monitor the temperature of the bulk fluid. This temperature is referred to as T_k (signifying its placement in the kettle). This thermocouple is placed well below the surface of the fluid. The other thermocouple (T2 in Fig. 2) is centered at the low point of distillate takeoff (the typical distillation head placement, as is carried out in classical distillations). The temperature measured directly in the fluid is a true state point that can be essential for modeling studies and comparison with theory. The temperature measured at the bottom of the distillation head takeoff point is needed to compare ADC measurements with classical measurements that have been taken for the last century.

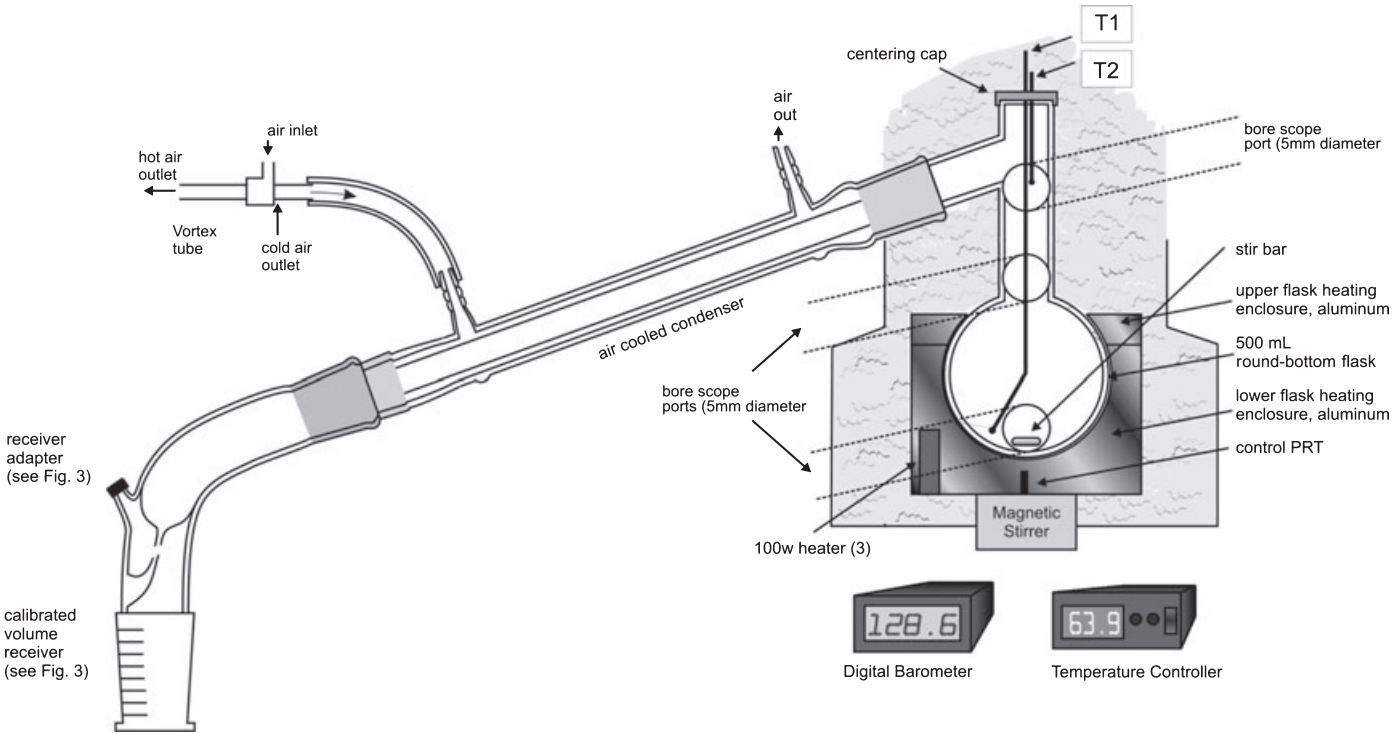

FIG. 2—*Schematic diagram of the overall apparatus used for the measurement of distillation curves. PRT, platinum resistance thermometer.*

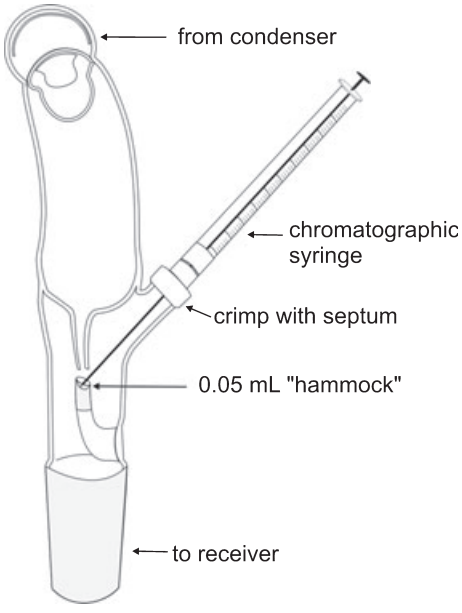

FIG. 3—*Schematic diagram of the receiver adapter to provide on-the-fly sampling of distillate cuts for subsequent analysis.*

Beneath the aluminum jacket, a magnetic stirrer drive is positioned to couple with a magnetic stir bar inside the distillation flask. Rapidly stirring the contents of the distillation flask during the measurement is essential for maintaining horizontal temperature uniformity in the fluid. The thermocouples positioned as aforementioned provide a rapid response to temperature. The uncertainty in the temperature measured with T2 in the distillation head is 0.1°C, while that of T1 in the fluid has been found to be somewhat lower at 0.05°C. We have found that the repeatability of temperatures in the distillation curve measurements on the same sample of ignitable liquid is *c*. 0.25°C over the entire curve.

Vaporized fluid taken from the flask is directed into a forced-air condenser chilled with a vortex tube (36). The vortex tube can produce a cold air stream to a temperature as low as −40°C. Following the condenser, the distillate enters a transfer adapter that allows instantaneous sampling of distillate for chemical analysis. To sample the distillate, one simply uses a chromatographic syringe equipped with a blunt-tipped needle, as shown in Fig. 3. The composition explicit data channel allows the use of any applicable analytical technique. The most common technique that is applied is gas chromatography with mass selective detection (GC–mass spectrometry (MS)). We have also augmented this with online Fourier transform infrared spectrophotometry (FTIR) utilizing a light pipe (GC–MS–FTIR), but more commonly we have applied FTIR offline. Specific element analysis has been applied for sulfur with a sulfur chemiluminescence detector. The sulfur analysis has been coupled with corrosivity analysis with a small scale copper strip corrosion test (37,38). We have also applied Karl Fisher coulombic titrimetry and refractometry in specific cases.

When the sample drops from the sampling transfer adapter, it flows into a level-stabilized receiver to allow a volume measurement shown in Fig. 4. This receiver consists of a central volume that gradually decreases in diameter at the base and connects to a smaller diameter side arm sight glass that is calibrated. The side arm stabilizes the fluid level for a precise volume measurement as the distillation proceeds. The large inner volume and the sight glass are enclosed in a water jacket that contains a thermometer and a magnetic stir bar for circulation. The side arm sight glass allows a volume measurement with an uncertainty of 0.05 mL. To perform a measurement, the fluid to be measured is placed in the round-bottom flask, and the thermocouples are placed in the appropriate positions. The temperature controller is programmed to apply a temperature profile to the distillation flask enclosure such that the

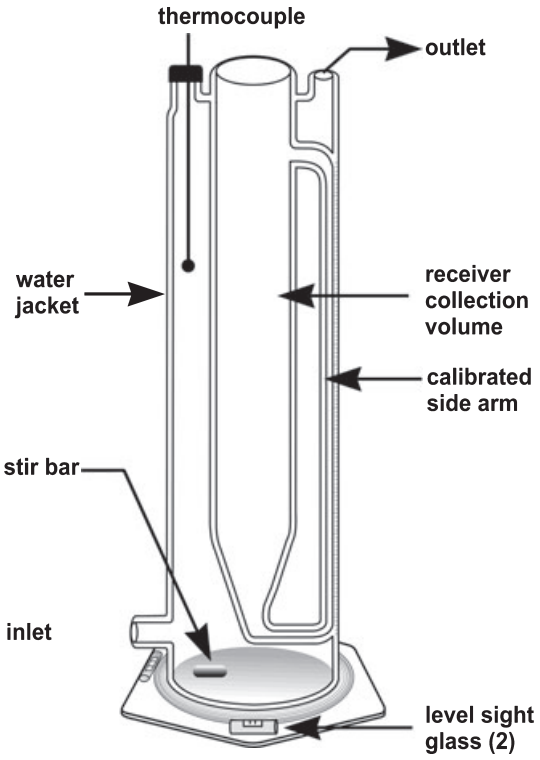

FIG. 4—*Schematic diagram of the level-stabilized receiver for distillation curve measurement.*

enclosure temperature leads the fluid temperature by some preselected temperature, for example 20°C. This is called model predictive control, and the use of it produces a constant mass flow rate through the distillation head. Moreover, the measured head temperature will be unaffected by rate aberrations that are commonly encountered in classical distillation curve measurement.

Because the ADC apparatus is operated at ambient atmospheric pressure, adjustments to standard sea level pressure must be made in the boiling temperatures that are recorded. This is done with a modification of the Sydney Young equation (39–42). Our modification to the classical equation is the use of a material-dependent proportionality constant. We typically present the adjusted temperatures and the measured atmospheric pressure so that the actual experimental temperature can be easily recovered.

TABLE 1—*A listing of fluids for which the ADC metrology has been applied.*

Sample (References)
Crude oils
Bohai bay crude (64)
Surmount oil sands crude (64)
Bio-crude oil from pig manure (61)
Rocket kerosenes
RP-1 (multiple lots) (19,44,45)
RP-2 (19,44,45)
TS-5 (19,44,45)
JP-10 (65)
Turbine fuels
Jet-A (multiple lots) (31,66)
JP-8 (USAF flight line sample) (63)
S-8 other natural gas synthetics (19)
JP-900 (CDF) (63)
Diesel fuels (67,68)
On-road diesel fuel*
Off-road diesel fuel†
Diesel fuel oxygenate mixtures
Tri(propylene glycol) methyl ether
Dibutyl maleate
Dibutyl fumarate
Dibutyl succinate
Cetaner‡
Dimethyl carbonate
Diethyl carbonate
γ-valerolactone
Biodiesel fuels (35,57–59)
B20 (35,57–59)
B100 (multiple lots) (35,57–59)
B100 with stabilizers§ (35,57–59)
Motor gasolines (30,69,70)
Summer quarter
Winter quarter
Constituent azeotropes
Fuel ethanol
Gasoline oxygenate mixtures
Methanol
E20
E85
γ-valerolactone
Aviation gasolines
Avgas 100LL (53)

*Green dye.
†Red dye.
‡An 80/20 (vol/vol) mixture of diethylene glycol methyl ether (DGME), +1,2-dimethoxyethane (DME).
§Stabilizers include hydrogen donors tetrahydroquinoline, *trans*-decahydronaphthalene, and tetralin.

Results and Discussion

Applications of the ADC in Characterizing Ignitable Liquids

As mentioned above, the ADC method can be used to provide predicted evaporation patterns for ignitable liquids and liquid residues encountered as ignitable liquids in cases of suspected arson. These data can be generated quickly, with a typical measurement requiring less than 1 h and the analyses requiring *c*. 4 h. There is less need for time-consuming ignitable liquid weathering studies. Moreover, the added credibility of the thermodynamically consistent temperature data, and the potential to describe the data with a model based on an equation of state, is also invaluable.

In Table 1, a listing of the fluids for which measurements have been taken thus far is provided, along with the appropriate reference. Many of the fluids listed have been used as ignitable liquids in arson fires. Clearly, the most common ignitable liquid on the list is gasoline, and we have measured numerous gasoline-based samples in the course of our fuels work (30). In the following description, we focus on other, less common fluids as they will allow the illustration of the more informative features of the ADC. Moreover, gasoline is already well studied and might be of less interest from a research perspective.

We anticipate that the practicing forensic scientist or criminalist will use the ADC in one of two ways. First, it will be possible to consult the published data (summarized in Table 1) that are available for predictions of the evaporation patterns of a suspected ignitable liquid. These data can be used predictively or to validate conclusions. Second, if an unusual ignitable liquid is suspected in a fire, the criminalist can use the ADC to rapidly generate the expected evaporation pattern. In either case, the ADC does not replace the usual analyses (such as GC–MS), but rather enhances or supplements them.

Rocket Kerosene

For each of the fluids in Table 1, the distillation curve points, consisting of temperature–volume fraction pairs, provide a measure

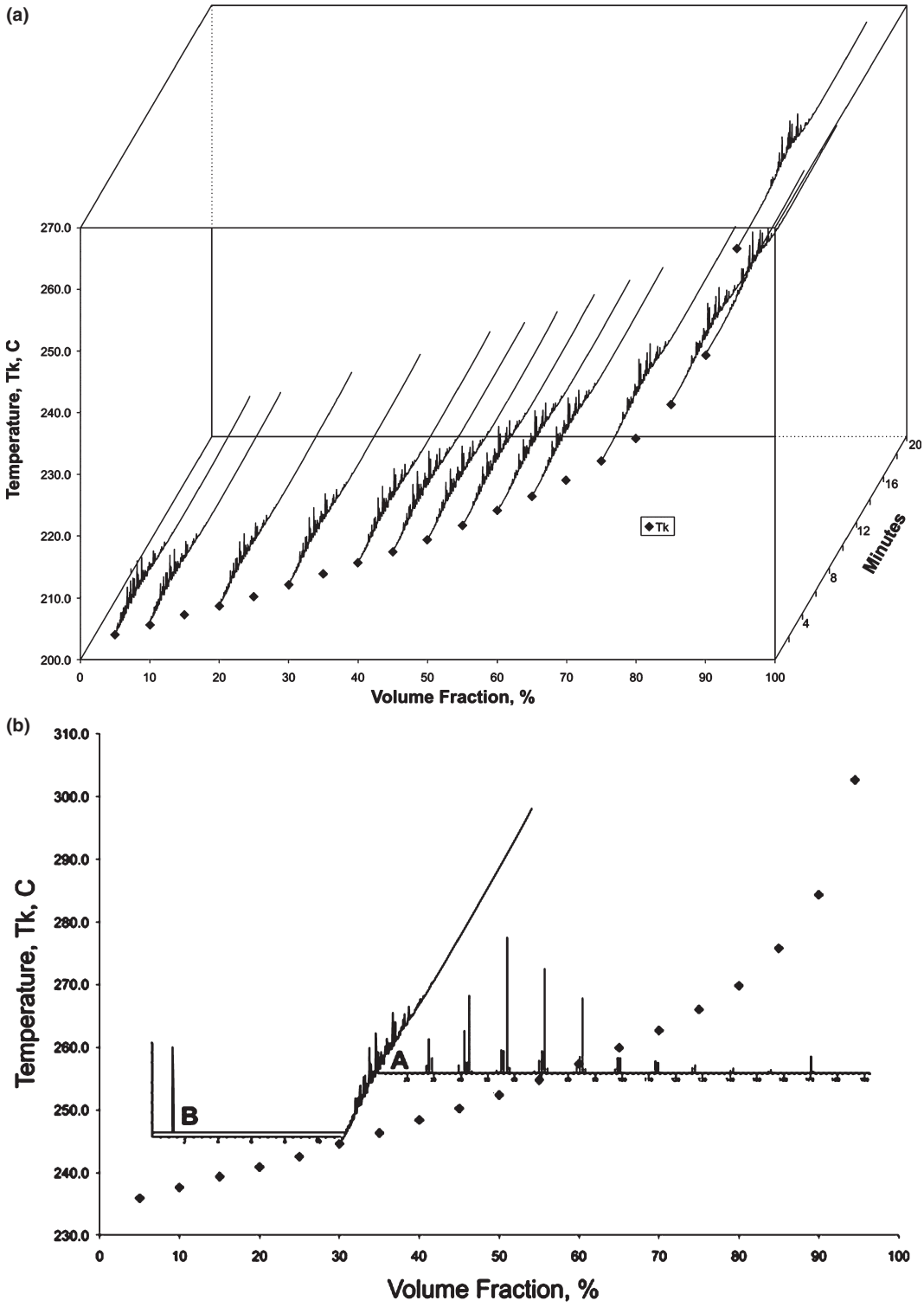

FIG. 5—*(a) A figure showing the measured distillation curve of RP-1, a modern rocket kerosene, with superimposed chromatographic analyses corresponding to selected temperature–volume fraction pairs. (b) The distillation curve of RP-1, in which for the 35% distillate volume fraction the largest peak in the chromatogram is identified as n-dodecane on the basis of its mass spectrum (A), and in which the total sulfur content is measured with a sulfur chemiluminescence detector (B).*

of fuel volatility. In addition, for each temperature–volume fraction pair, we also have a chemical analysis, as shown in Fig. 5*a* for RP-1, a kerosene that is used as a rocket propellant (19,43,44). Here, on the "z" axis, are total ion chromatograms (obtained by GC–MS) for the samples taken at each of the indicated distillate fractions. One can see that the typical kerosene pattern emerges for all the samples, but the changing composition trend is clear as the distillation (or evaporation) proceeds. The early fractions are rich in the lighter components, and as the distillation progresses to higher volume fractions, the chromatograms are shifted to the heavier

components that boil at higher temperatures. This is important in the fundamental description of fluid behavior because it is this changing suite of components that determines the profile of the distillation curve. It is also significant in that it provides essentially the same evaporation profile that would be expected in the analysis of fire debris exposed to varying high temperatures.

The information in Fig. 5*a* can be augmented, again as a function of distillate volume fraction, with any analytical technique that can be applied to a fluid sample. Moreover, these techniques can be applied after a chromatographic separation. In Fig. 5*b*, we present the same distillation curve for RP-1, but focusing only on the 35% distillate volume fraction. We demonstrate how mass spectrometry can be used to identify the peaks in the spectrum; in the inset (A), the largest peak is identified as n-dodecane on this basis. We can also apply element-specific analyses if desired. In inset (B), we demonstrate how sulfur chemiluminescence can be used to determine the total sulfur content of that distillate fraction. As applied to ignitable liquids, therefore, one cannot only rapidly determine the predicted evaporation profile but also characterize the constituents (including those at trace levels) in terms of species and concentrations. The chromatographic profiles resulting from the ADC can be demonstrated with greater clarity by reference to Fig. 6, in which the chromatographic results of the 0.025%, 10%, 50%, and 90% distillate volume fractions (presented top to bottom) of rocket kerosenes RP-1, RP-2, and TS-5 (presented left to right) are shown (44,45). This work was carried out with a GS–MS–FTIR method (30-m capillary column of 5% phenyl dimethyl polysiloxane, having a thickness of 1 μm, temperature program from 90 to 250°C, 10°C/min). Mass spectra were collected for each peak from 15 to 550 relative molecular mass units, and infrared spectra were collected between 4000 and 600/cm (46,47). Only the total ion chromatograms obtained from the mass spectrometer are presented. The information from the FTIR is valuable nonetheless, especially in distinguishing the kerosene from any pyrolysis products. The pyrolysis products of both common substrates and rocket kerosenes often contain naphthalenics and complex aromatics, and FTIR is useful for confirming GC–MS results (48–52). The series of chromatograms is predictive of the evaporation pattern that can be expected at atmospheric pressure for the kerosene.

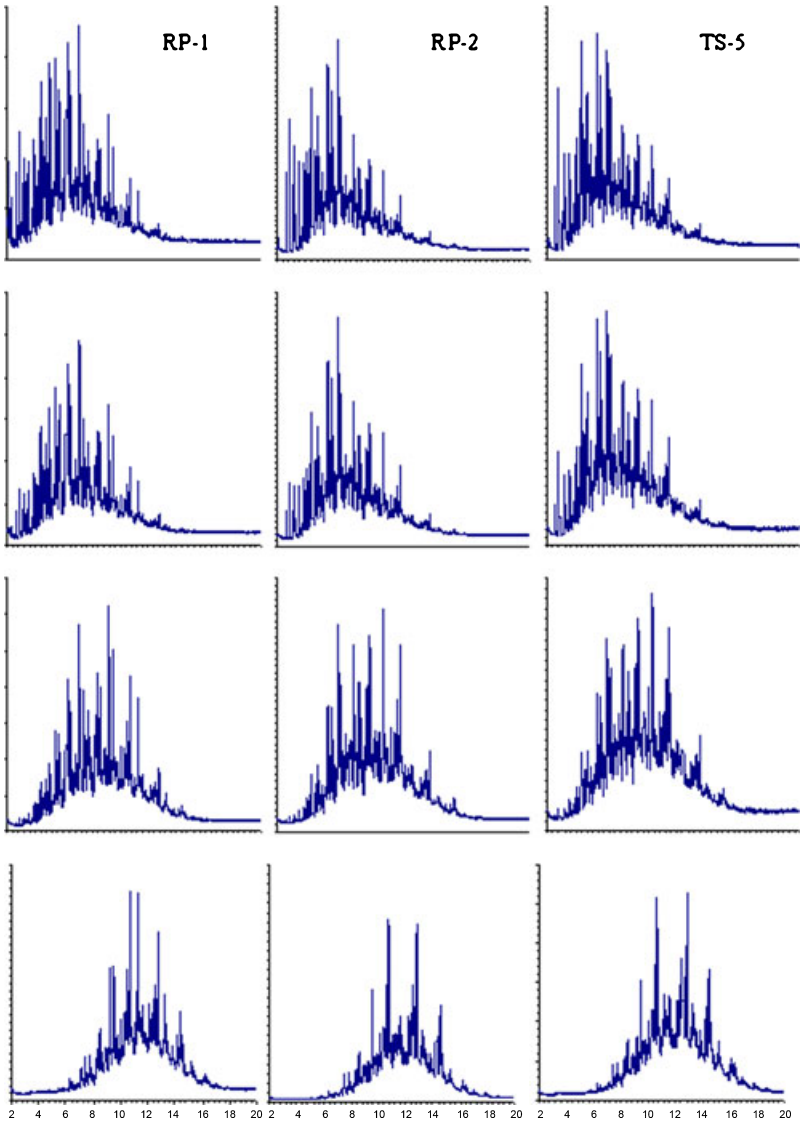

FIG. 6—*A series of total ion chromatograms of the 0.025%, 10%, 50%, and 90% distillate volume fractions (presented top to bottom) of RP-1, RP-2, and TS-5 (presented left to right). The similarity to the evaporation patterns of Fig. 1 is striking.*

Aviation Gasoline

We illustrate additional features of the ADC approach in Fig. 7, in which a curve for general aviation gasoline, avgas 100LL, is shown (53). Some preliminary comments about avgas in general and this sample of avgas in particular will assist in describing the features in this figure. In the past, aviation gasoline grades were differentiated by the two numbers following the general name avgas (e.g., avgas 80/87, avgas 115/145, and avgas 100/130) (54). The different fuels were differentiated in the field by a dye that colored the fluid. Thus, avgas 80/87 (phased out in the early 1990s) was colored red, avgas 115/145 (primarily used earlier in the military) was colored purple, avgas 100/130 (now available mainly in Australia and New Zealand) was colored green, and avgas 100LL was colored blue. The first number indicated how the fuel behaves under load and is the aviation lean octane rating, which is very close to the more familiar Motor Octane Number (MON) commonly specified for automotive applications. The second number indicated how the fuel behaves at takeoff and is the aviation rich octane rating. Currently, only the aviation lean octane rating is used to specify avgas grades (e.g., avgas 100LL and avgas 82UL). Here, LL and UL refer to low lead and unleaded, respectively. Lead compounds (primarily, tetraethyl lead, TEL, CAS No. 78-00-2) are additives used to improve the MON. For 100LL, the lead concentration is specified as an upper limit of 0.56 g of TEL per liter of fuel.

A representative ADC measurement for avgas 100LL is shown in Fig. 7. The composition explicit data channel provides an avenue to many additional properties of the fuel that are relevant to fire debris analysis. The chromatograms obtainable at each fraction allow for not simply pattern recognition but also qualitative and quantitative analyses. The chromatographic peaks for each fraction on Fig. 7 can be identified from the individual mass spectra or infrared spectra. Moreover, one can use various calibration methods to quantify each peak. If GC–MS or GC–MS–FTIR is not the preferred technique for the quantitative analysis, it is a simple matter to repeat the analyses with a flame ionization detector. Thus, for a complex fuel chromatogram, one can calibrate, for example, the constituents present at a particular threshold. In our fuel analysis work, we typically identify and quantify all peaks above 1% (mol/mol). This allows the construction of a table of compounds for each volume fraction, along with the molar concentration. From this, any concentration-based property may be inferred; the uncertainties in these determinations have been discussed in detail elsewhere (28). For example, one can then use the pure component enthalpy of combustion to determine an overall enthalpy of combustion for each fraction. This is illustrated for avgas 100LL in inset (a) of Fig. 7. This allows the calculation of the energy content of each fraction, and because this is related to the evaporation pattern so important to fire debris analysts, an estimate of the energy released (or rather, available for reaction) by the ignitable liquid prior to sample collection. One can also estimate the quantity of energy remaining in any recovered ignitable liquid.

In addition to standard qualitative and quantitative analyses, trace analyses are possible with the composition channel. As aforementioned, avgas 100LL contains the additive TEL. We can analyze for the presence of this additive as a function of distillate cut, as shown in inset (b) in Fig. 7. This analysis was carried out by GC–MS, using selected ion monitoring of characteristic peaks at the m/z values 208, 237, and 295. We note that the TEL is present in all distillate cuts except the very first drop. In the early stages of the distillation, the concentration is very low, and this is observed to increase by approximately the half-way point. The concentration is highest at the later stages of the distillation. This is entirely consistent with what one would expect from evaporation or weathering studies, because early in the distillation the quantity of TEL recovered relative to the other avgas constituents is indeed very low. As evaporation (or weathering) of the sample occurs, the TEL concentration relative to the other components is observed to increase.

The relationship of the composition channel of the ADC and the evaporation profile that a criminalist might expect to find in fire debris is illustrated clearly with this example. A fire that has caused a piece of recovered debris to reach an internal temperature consistent with the latter stages of the distillation curve will show a pattern that is predictable by the ADC method. Such identification is

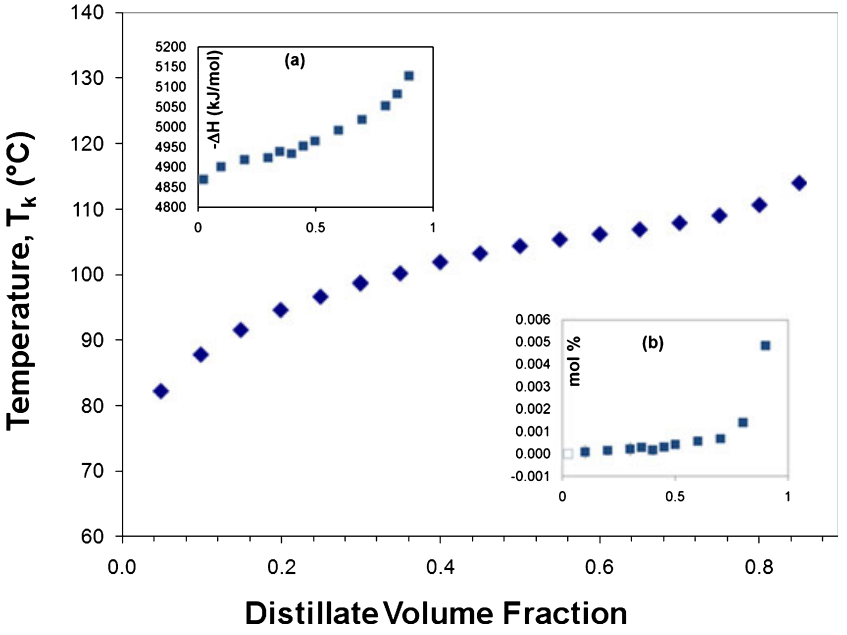

FIG. 7—*The distillation curve of aviation gasoline, Avgas 100LL. Inset (a) shows the enthalpy of combustion as a function of distillate volume fraction; inset (b) shows the molar concentration of TEL as a function of distillate cut.*

often possible, as many fire debris samples (in which gasoline was used as an ignitable liquid) are recovered in which evaporation is between 40% and 60% (15). Along with this predicted evaporation profile, one can obtain a prediction of a trace constituent that may be able to function as a de-facto taggent under some circumstances, and this has been noted by other workers (13,55,56). While such a statement does not imply a recommendation to re-introduce TEL into gasoline for use as a taggent, it does open the possibility of adding an acceptable taggent to fuels used by first responders. As is well known, firefighters using gasoline-powered equipment must often refuel such equipment at the fire scene (6,7). When a fire scene later becomes a crime scene, the contamination of the scene (actual or alleged) with gasoline often becomes an issue in court. The use of a tagged fuel, along with the predicted evaporation data from the ADC, can make subsequent fire debris analysis less uncertain and less liable to challenge. One could differentiate the tagged fuel from untagged fuel with relative ease. Moreover, this could be performed by reference to a reliable database of fuel properties provided by the ADC, rather than with numerous time-consuming weathering studies.

Biodiesel Fuel

We mentioned earlier that a study has been carried out anticipating the occurrence of biodiesel fuel as an ignitable liquid (8). In our work on fuel properties, we have used the ADC to measure numerous biodiesel fuels and mixtures in which biodiesel fuel is the base fluid (57–59). The main components of neat biodiesel fuel, referred to as B100, are surprisingly simple. In order of elution on a polar gas chromatographic column, one finds the fatty acid methyl esters (FAMEs): methyl palmitate (hexadecanoic acid, methyl ester; CAS 112-39-0), methyl stearate (octadecanoic acid, methyl ester; CAS 112-61-8), methyl oleate (octadecenoic acid, methyl ester; CAS 112-62-9), methyl linoleate (octadecadienoic acid, methyl ester; CAS 112-63-0), and methyl linolenate (octadecatrienoic acid, methyl ester; CAS 301-00-8) (60). Other related compounds are of course present, but at much lower concentrations. Although B100 is commercially available, most biodiesel fuel used for motor applications is mixed with petroleum-derived ultra-low sulfur diesel fuel (ULSD) to produce B05 (5%, vol/vol, biodiesel fuel with ULSD) or B20 (20%, vol/vol, biodiesel fuel with ULSD). The ADC technique has been applied to these various fluids, along with the compositional and enthalpic data as described above. Especially relevant to the prediction of evaporation patterns that might be observed in fire debris are the example chromatograms presented in Fig. 8*a,b*.

In Fig. 8*a*, we present the chromatograms from the 0.025%, 10%, 50%, and 80% distillate volume fractions of B20. The analyses were carried out by gas chromatography with mass spectral detection (30-m capillary column with a 0.1 mm coating of 50% cyanopropyl–50% dimethylpolysiloxane, split/splitless injector set with a 50–1 split ratio, injector operated at of 325°C and a constant head pressure of 10 psig). We note for the first fraction at 0.025%, the chromatogram is dominated by the tail end of the kerosene pattern of the ULSD, while the bio-derived components are present late in the chromatogram and at comparatively lower levels (the shaded area). As the chromatograms progress to later distillate fractions, we note that the bio-derived components increase in relative concentration and finally dominate by the 80% distillate fraction. These patterns are predictive of what would be observed in the evaporation pattern. A sample of B20 exposed to elevated temperatures in a fire would predominantly show the FAME fraction, with traces of the petroleum-derived fraction present at a much lower concentration that would be found in the finished fuel. In an analogous fashion, in Fig. 8*b* we provide the chromatograms for the same distillate fractions of B100. We note the familiar diesel fuel pattern in the very first fraction. This is because there is at present always some ULSD in B100 stock owing to tank contamination. Then, as the distillation proceeds, we note only the FAME fraction, with the heavier FAMEs increasing and the lighter ones decreasing. These predicted patterns will be valuable in the identification of B20 and B100 in fire debris.

Residue Analysis

An aspect of the ADC that we have not discussed earlier is that one will often note the presence of a residual solid after the distillation measurement is complete. This aspect of the ADC presents the opportunity to apply additional analytical methods to the sample. We can discuss as an example a bio-crude oil made from the heat treatment of swine manure as a fluid with a significant dissolved or suspended solids content (61). Upon completion of the distillation, a solid residue was recovered from the distillation flask. This material, which contained unreacted manure solids, was analyzed by X-ray methods (diffraction and fluorescence), instrumental neutron activation analysis, and cold neutron prompt gamma activation analysis (CN-PGAA). These latter complementary neutron activation analysis techniques detected the presence of the following heavy metals in the solid: Fe, Zn, Ag, Co, Cr, La, Sc, W, and very small amounts of Au and Hf. These analyses allowed conclusions to be drawn concerning the feedstock. As the heavy metals could not be thermo-converted into the bio-crude oil, they were largely indicative of the diet and mineral supplement budget of the swine used in the research. This has relevance in the prediction and analysis of ignitable liquid in fire debris. For example, criminalists commonly suspect the use of turpentine as an ignitable liquid, and they must determine whether the turpentine is natural or an ignitable liquid (62). Residue analysis subsequent to a measurement with the ADC has the potential of simplifying such determinations and can even provide an indication of the source of the trees from which the turpentine was manufactured (M. Higgins, personal communication). This is analogous to our interpretation of the CN-PGAA results discussed earlier.

Thermodynamic Modeling

We have mentioned several times that an important advantage provided by the ADC is the ability to predict the distillation curve with a thermodynamically based equation of state. Our use of the term "predict" in this context is very different from the usage we have made above in the discussion of predicted evaporation patterns. When discussing the evaporation patterns, we noted that the composition explicit data channel of the ADC essentially provided the compositional suite of products that is obtained in weathering studies, because the mechanism (evaporation or vaporization) is the same. We therefore use a simple experimental approach to predict what would be obtained in a relatively time-consuming experimental approach. In the context of an equation of state prediction, we use thermodynamic theory to calculate a result. In this context, the term "predict" merely indicates that the experimental verification of the calculation is not necessarily performed or available.

In our work on fuels, we have found that models based on the Helmholtz free energy equation of state offer many important advantages; thus, this is the approach that we use. While a fundamental description of this theory is beyond the scope of this article,

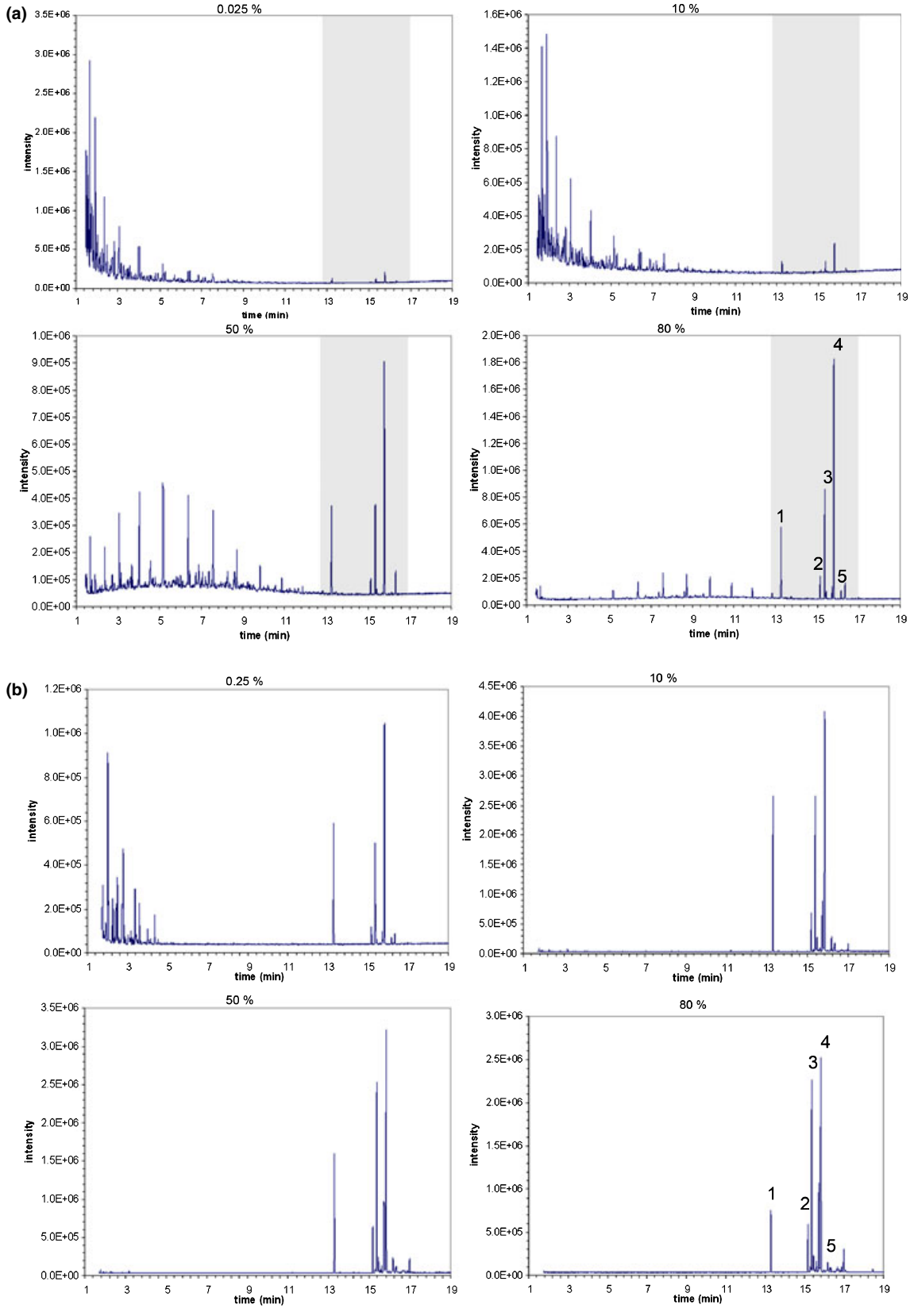

FIG. 8—*(a) Chromatograms of distillate fractions of B20, presented in arbitrary units of intensity, of the 0.025%, 10%, 50%, and 80% volume fractions. The five main biodiesel fatty acid methyl ester (FAME) peaks are labeled: 1, methyl palmitate; 2, methyl stereate; 3, methyl oleate; 4, methyl linoleate; 5, methyl linolenate. (b) Chromatograms of distillate fractions of B100, presented in arbitrary units of intensity, of the 0.025%, 10%, 50%, and 80% volume fractions. The five main biodiesel FAME peaks are labeled: 1, methyl palmitate; 2, methyl stereate; 3, methyl oleate; 4, methyl linoleate; 5, methyl linolenate.*

we can describe an example of the applications. Another fuel on Table 1 that we have characterized with the ADC is a prototype JP-900 aviation fuel (63). This is a coal-derived alternative gas turbine fuel that was formulated to be thermally stable up to 900°F (hence the designation). We developed a surrogate model (based on representative model compounds) with the Helmholtz equation of state to predict most of the thermophysical properties of that fluid, including the distillation curve (33). In Fig. 9, we compare the measured curve to the prediction. We note that the curve can be calculated theoretically to within experimental uncertainty. At any stage of the calculation, it is possible to recover the predicted fluid composition, thus offering the potential of calculating the evaporation pattern that might be expected. While this aspect of the application of the ADC to fire debris analysis is the least developed, the results are very promising and further work is ongoing.

Conclusion

In this paper, we have described how the suite of measurements included in the ADC protocol can be used to predict the evaporation patterns of ignitable liquids that are recovered in fire debris subsequent to arson fires, and thereby enhance conclusions derived from techniques, such as GC–MS. The utility of this method extends beyond providing simple chromatographic patterns, but can include quantitative analysis and trace analysis, as well as enthalpic analysis of samples. We emphasize that the ADC is not proposed as a replacement for all weathering or ignitable liquid evaporation studies, but we argue that it can be used to supplement or extend information derived from such studies. Moreover, the forensic science community can benefit by tapping into the body of such data that is already measured (or currently being measured) in the course of studying fuel properties. The ADC can be especially useful to the criminalist when an unusual or uncommon ignitable liquid is encountered, for which the evaporation characteristics might be unknown. The approach also has application in rapidly assessing the compositional variability of a family of ignitable liquids, such as paint thinners, as valid predictions can be obtained in a short time. Moreover, a criminalist can use the ADC to quickly and easily generate reference evaporation patterns to compare with analytical results from fire debris. The relationship of those evaporation patterns to the fluid equations of state can provide a new dimension of reliability to expert testimony. In the future, our experimental work will include ignitable liquids, such as paint thinners and industrial solvents, and we expect to continue development of the thermodynamic modeling approach to the calculation of evaporation profiles.

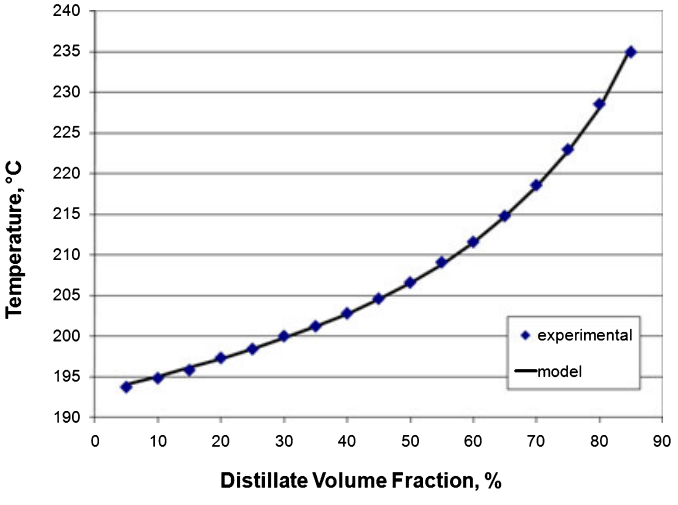

FIG. 9—*Comparison of a measured curve from the advanced distillation curve approach for a coal derived aviation fuel, JP-900, with that predicted with the Helmholtz free energy equation of state.*

Conflict of interest: The authors have no relevant conflicts of interest to declare.

Acknowledgment

Financial support received from the Air Force Research Laboratory (MIPR F1SBAA8022G001).

References

1. Hine GA. Fire scene investigation: an introduction for chemists. In: Almirall JR, Furton KG, editors. Analysis and interpretation of fire scene evidence. Boca Raton, FL: CRC Press, 2004;33–75.
2. Lentini JJ. The standard of care in fire investigation. 2009, http://www.innocencenetwork.org/docs/Lentini (accessed September 15, 2009).
3. Other disputed arson cases, innocence project, Benjamin Cardozo School of Law, Yeshiva University, innocenceproject.org. New York, NY: Innocence Project, Inc., 2009.
4. Carpenter DJ, Churchward DL, Lentini JJ, McKenzie MA, Smith DM. Report on the peer review of the expert testimony on cases of *State of Texas v. Cameron Todd Willingham* and *State of Texas v. Ernest Ray Willis*. Arson Review Committee: A Peer Review Panel Commissioned by the Innocence Project. New York, NY: Innocence Project, Inc., 2006.
5. Al-Kandary JAM, Al-Jimaz ASH. Study on blends of crude oil with sludge left in Kuwaiti oil lakes. Pet Sci and Tech 2000;18(7&8):795–814.
6. NFPA. Guide for fire and explosion investigations, NFPA 921. Quincy, MA: National Fire Prevention Association, 2004.
7. Sandercock MPL. Fire investigation and ignitable liquid residue analysis—a review: 2001–2007. Forensic Sci Int 2008;176:93–110.
8. Stauffer E, Byron D. Alternative fuels in fire debris analysis: biodiesel basics. J Forensic Sci 2007;52(2):371–9.
9. DeVos BJ. Gas chromatography coupled with ion trap mass spectrometry (GC-MS and GC-MS-MS) for arson debris analysis [dissertation]. Pretoria, South Africa: University of Pretoria, 2005.
10. Pert AD, Baron MG, Birkett JW. Review of analytical techniques for arson residues. J Forensic Sci 2006;51(5):1033–49.
11. Rella R, Sturato A, Parvoli G, Ferrara D, Doretti L. Ignitable liquid identification in fire debris by TCT-GC-MS. LC-GC Europe 2002; September:2–6.
12. Dolan J. Analytical methods for the detection and characterization of ignitable liquid residues from fire debris. In: Almirall JR, Furton KG, editors. Analysis and interpretation of fire scene evidence. Boca Raton, FL: CRC Press, 2004;137–65.
13. Hirz R. Gasoline brand identification and individualization of gasoline lots. J Forensic Sci Soc 1989;29(2):91–101.
14. Jayatilaka A, Poole CF. Identification of petroleum distillates from fire debris using multidimensional gas chromatography. Chromatographia 1994;39(3/4):200–9.
15. Mann DC. Comparison of automotive gasolines using capillary gas chromatography II: limitations of automotive gasoline comparisons in casework. J Forensic Sci 1987;32(3):616–28.
16. Tan B, Hardy JK, Snavely RE. Accelerant classification by gas chromatography mass spectrometry and multivariate pattern recognition. Anal Chim Acta 2000;422:37–46.
17. Wallace JR. GC/MS data from fire debris samples: interpretation and applications. J Forensic Sci 1999;44(5):996–1012.
18. Bruno TJ. Improvements in the measurement of distillation curves—part 1: a composition-explicit approach. Ind Eng Chem Res 2006;45:4371–80.
19. Bruno TJ, Smith BL. Improvements in the measurement of distillation curves—part 2: application to aerospace/aviation fuels RP-1 and S-8. Ind Eng Chem Res 2006;45:4381–8.
20. Bruno TJ. Method and apparatus for precision in-line sampling of distillate. Sep Sci Technol 2006;41(2):309–14.
21. Smith BL, Bruno TJ. Advanced distillation curve measurement with a model predictive temperature controller. Int J Thermophys 2006;27:1419–34.

22. ASTM International. ASTM Standard D 86-04b, standard test method for distillation of petroleum products at atmospheric pressure. West Conshohocken, PA: ASTM International, 2004.
23. Kister HZ. Distillation operation. New York, NY: McGraw-Hill, 1988.
24. Kister HZ. Distillation design. New York, NY: McGraw-Hill, 1991.
25. Riazi MR, Al-Adwani HA, Bishara A. The impact of characterization methods on properties of reservoir fluids and crude oils: options and restrictions. J Petrol Sci Eng 2004;42(2-4):195–207.
26. Organisation for Economic Co-operation and Development (OECD). OECD guideline for the testing of chemicals, No. 103, boiling point (adopted by the Council, July 27). Paris, France: Organisation for Economic Co-operation and Development, 1995.
27. Purchase Description, RP-1, Federal Business Opportunities, 2003, http://fs2.eps.gov/EPSData/DLA/Synopses/12671/SP0600-03-R-0322/rp-1sol.pdf (accessed September 15, 2009).
28. Bruno TJ, Smith BL. Enthalpy of combustion of fuels as a function of distillate cut: application of an advanced distillation curve method. Energy Fuels 2006;20:2109–16.
29. Ott LS, Bruno TJ. Corrosivity of fluids as a function of distillate cut: application of an advanced distillation curve method. Energy Fuels 2007;21:2778–84.
30. Smith BL, Bruno TJ. Improvements in the measurement of distillation curves: part 3—application to gasoline and gasoline + methanol mixtures. Ind Eng Chem Res 2007;46:297–309.
31. Smith BL, Bruno TJ. Improvements in the measurement of distillation curves: part 4—application to the aviation turbine fuel Jet-A. Ind Eng Chem Res 2007;46:310–20.
32. Huber ML, Smith BL, Ott LS, Bruno TJ. Surrogate mixture model for the thermophysical properties of synthetic aviation fuel S-8: explicit application of the advanced distillation curve. Energy Fuels 2008;22:1104–14.
33. Huber ML, Lemmon EW, Diky V, Smith BL, Bruno TJ. Chemically authentic surrogate mixture model for the thermophysical properties of a coal-derived-liquid fuel. Energy Fuels 2008;22:3249–57.
34. Huber ML, Lemmon E, Kazakov A, Ott LS, Bruno TJ. Model for the thermodynamic properties of a biodiesel fuel. Energy Fuels 2009;23:3790–7.
35. Huber ML, Lemmon E, Ott LS, Bruno TJ. Preliminary surrogate mixture models for rocket propellants RP-1 and RP-2. Energy Fuels 2009;23:3083–8.
36. Bruno TJ. Vortex cooling for subambient temperature gas chromatography. Anal Chem 1986;58(7):1595–6.
37. Andersen WC, Straty GC, Bruno TJ. Improving the copper strip corrosion test. Proceedings of the GTI natural gas technologies II conference and exhibition; 2004 Feb 8-11; Phoenix, AZ. Des Plaines, IL: Gas Technology Institute, 2004.
38. Ott LS, Bruno TJ. Modifications to the copper strip corrosion test for the measurement of microscale samples. J Sulfur Chem 2007;28(5):493–504.
39. Ott LS, Smith BL, Bruno TJ. Experimental test of the Sydney Young equation for the presentation of distillation curves. J Chem Thermodynam 2008;40:1352–7.
40. Young S. Correction of boiling points of liquids from observed to normal pressures. Proc Chem Soc 1902;81:777.
41. Young S. Fractional distillation. London, UK: Macmillan and Co., Ltd., 1903.
42. Young S. Distillation principles and processes. London, UK: Macmillan and Co., Ltd., 1922.
43. Dean LE, Shirley LA. Characteristics of RP-1 rocket propellant. Sacramento, CA: Aerojet General Corp., 1957. Report No.: Technical Report TCR-70.
44. Ott LS, Hadler A, Bruno TJ. Variability of the rocket propellants RP-1, RP-2, and TS-5: application of a composition- and enthalpy-explicit distillation curve method. Ind Eng Chem Res 2008;47(23):9225–33.
45. Lovestead TM, Bruno TJ. Comparison of the hypersonic vehicle fuel JP-7 to the rocket propellants RP-1 and RP-2 with the advanced distillation curve method. Energy Fuels 2009;23(7):3637–44.
46. Bruno TJ, Svoronos PDN, editors. CRC handbook of basic tables for chemical analysis, 2nd edn. Boca Raton, FL: Taylor and Francis CRC Press, 2004.
47. Bruno TJ, Svoronos PDN. CRC handbook of fundamental spectroscopic correlation charts. Boca Raton, FL: Taylor and Francis CRC Press, 2005.
48. Stauffer E. Sources of interference in fire debris analysis. In: Nic Daeid N, editor. Fire investigation. Boca Raton, FL: CRC Press, 2004;371–9.
49. Widegren JA, Bruno TJ. Thermal decomposition kinetics of kerosene based rocket propellants 2 RP-2 stabilized with three additives. Energy Fuels 2009;23(11):5523–8.
50. Andersen PC, Bruno TJ. Thermal decomposition kinetics of RP-1 rocket propellant. Ind Eng Chem Res 2005;44(6):1670–6.
51. Widegren JA, Bruno TJ. Thermal decomposition of RP-1 and RP-2, and mixtures of RP-2 with stabilizing additives. Proceedings of 4th Liquid Propulsion Subcommittee; 2008 Dec 8-12; Orlando, FL. Baltimore, MD: Joint Army-Navy-NASA-Air Force (JANNAF), 2008.
52. Widegren JA, Bruno TJ. Thermal decomposition kinetics of kerosene based rocket propellants 1. Comparison of RP-1 and RP-2. Energy Fuels 2009;23(11):5517–22.
53. Lovestead TM, Bruno TJ. Application of the advanced distillation curve method to aviation fuel avgas 100LL. Energy Fuels 2009;23:2176–83.
54. Visser B. Autogas vs. avgas: the differences can be major if not properly managed. Gen Aviat News 2004;1:1.
55. Chan I. The determination of tetraalkyl lead compounds in petrol using combined gas chromatography atomic absorption spectrometry. Forensic Sci Int 1981;18:57–62.
56. Frank HA. Lead alkyl components as discriminating factors in the comparison of gasolines. J Forensic Sci 1980;20(4):285–92.
57. Bruno TJ, Wolk A, Naydich A. Stabilization of biodiesel fuel at elevated temperature with hydrogen donors: evaluation with the advanced distillation curve method. Energy Fuels 2009;23:1015–23.
58. Ott LS, Bruno TJ. Variability of biodiesel fuel and comparison to petroleum-derived diesel fuel: application of a composition and enthalpy explicit distillation curve method. Energy Fuels 2008;22:2861–8.
59. Smith BL, Ott LS, Bruno TJ. Composition-explicit distillation curves of commercial biodiesel fuels: comparison of petroleum derived fuel with B20 and B100. Ind Eng Chem Res 2008;47(16):5832–40.
60. Ott LS, Huber ML, Bruno TJ. Density and velocity of sound measurements on five fatty acid methyl esters at 83 kPa and temperatures from (278.15 to 338.15) K. J Chem Eng Data 2008;53:2412–6.
61. Ott LS, Smith BL, Bruno TJ. Advanced distillation curve measurement: application to a bio-derived crude oil prepared from swine manure. Fuel 2008;87:3379–87.
62. Higgins M. Turpentine: ignitable liquid or natural. Fire Arson Invest 1987;38(2):10.
63. Smith BL, Bruno TJ. Composition-explicit distillation curves of aviation fuel JP-8 and a coal based jet fuel. Energy Fuels 2007;21:2853–62.
64. Ott LS, Smith BL, Bruno TJ. Advanced distillation curve measurements for corrosive fluids: application to two crude oils. Fuel 2008;87:3055–64.
65. Bruno TJ, Huber ML, Laesecke A, Lemmon EW, Perkins RA. Thermochemical and thermophysical properties of JP-10, NIST-IR 6640. Gaithersburg, MD: National Institute of Standards and Technology (U.S.), 2006.
66. Smith BL, Bruno TJ. Application of a composition-explicit distillation curve metrology to mixtures of Jet-A + Synthetic Fischer-Tropsch S-8. J Propul Power 2008;24(3):619–23.
67. Ott LS, Smith BL, Bruno TJ. Composition-explicit distillation curves of mixtures of diesel fuel with biomass-derived glycol ester oxygenates: a fuel design tool for decreased particulate emissions. Energy Fuels 2008;22:2518–26.
68. Smith BL, Ott LS, Bruno TJ. Composition-explicit distillation curves of diesel fuel with glycol ether and glycol ester oxygenates: a design tool for decreased particulate emissions. Environ Sci Tech 2008;42(20):7682–9.
69. Bruno TJ, Wolk A, Naydich A. Composition-explicit distillation curves for mixtures of gasoline with four-carbon alcohols (butanols). Energy Fuels 2009;23:2295–306.
70. Hadler AB, Ott LS, Bruno TJ. Study of azeotropic mixtures with the advanced distillation curve approach. Fluid Phase Equilib 2009;281:49–59.

Additional information and reprint requests:
Thomas J. Bruno, Ph.D.
Properties for Process Separations
Thermophysical Properties Division
National Institute of Standards and Technology
325 Broadway, MS 838.00
Boulder, CO 80305
E-mail: bruno@boulder.nist.gov